Fiber Bragg Grating Feedback System for Recurve Bows

Andrew Pignatelli
Engineering Physics
Final Project Report, 2024–2025
andrewpignatelli
@cmail.carleton.ca

Dr. Christopher Smelser
ChristopherSmelser
@CUNET.CARLETON.CA

This project investigates the integration of Fiber Bragg Grating (FBG) sensors into a recurve bow for real-time analysis during use. Utilizing the high sensitivity of FBG sensors, the system captures dynamic information related to strain and vibration. The collected wavelength data is processed through MATLAB to derive metrics such as draw strength and strain relationships, while a Python-based Graphical User Interface (GUI) visualizes this data in real time.
Results demonstrated differential compressive strain values of $-2033.\ \mu\varepsilon$ and $-2088.7\ \mu\varepsilon$ on the right and left sides of the upper limb. An MPU6050 module was included to provide supplementary directional and vibrational data, enabling motion-aware strain correlation.
This system addresses limitations in traditional archery analysis tools by introducing photonic sensing to dynamic sporting applications. The modular design supports future scalability, adaptability, and further integration with structural health monitoring systems.

Carleton University

CONTENTS

CHAPTER 1

INTRODUCTION

1.1 Project Introduction

This capstone project focuses on the development of a fiber-optic sensing system for the real-time analysis of a recurve bow during draw and release. By embedding Fiber Bragg Grating (FBG) sensors along both limbs and interrogating them with an Ibsen I-MON E interrogator, the system captures strain and vibrational signals with high spatial and temporal resolution. The raw spectral data are processed in MATLAB to extract precise Bragg wavelength shifts corresponding to mechanical deformation. An onboard MPU-6050 inertial measurement unit (IMU) provides 3-axis acceleration and orientation information. A custom graphical user interface visualizes draw strength, strain distribution, acceleration, and vibrational response in real time, delivering actionable feedback to archers and coaches.

This work brings photonic sensing which is traditionally reserved for structural health monitoring into a dynamic sports context, opening new areas for performance optimization and equipment evaluation. The high sensitivity, immunity to electromagnetic interference, and multiplexing capability of FBG sensors allow multiple measurement points along the bow without adding significant mass or wiring complexity. This project demonstrates a novel method for real-time feedback in archery and lays the groundwork for smart athletic equipment in sports engineering.

1.2 Literature Review

The design and development of the optical sensor system is based on several key references, which covers the theory of Fiber Bragg Gratings (FBGs) and practical implementation tools for data collection and analysis.

General Theory

- **Fiber Bragg Gratings – Raman Kashyap**
  This text provides a detailed explanation of the physics of FBG sensors, covering all of the theoretical and practical uses.

- **Fiber Bragg Gratings: Fundamentals and Applications in Telecommunications and Sensing – Andreas Othonos & Kyriacos Kalli**
  This book offers an applied perspective on the use of FBGs, particularly in sensing applications. It was used to better understand the operational behavior of FBGs in embedded environments and specifically supported the derivation of the equation used to determine strain.

- **Fiber Bragg Gratings: Theory and Practic - Marcelo Martins**
  This source helped reinforce the practical and theoretical knowledge needed to implement FBG sensors effectively.

Implementation References

- **Introduction to MATLAB for Engineers – William J. Palm III**
  This textbook was used for developing MATLAB scripts to process spectral data. Specifically, it aided in

filtering, visualizing, and extracting peak wavelength shifts from the I-MON data in order to determine strain behavior.

- **I-MON E Interrogator 512 User Manual**
  The official user manual for the Ibsen Photonics I-MON spectrum analyzers provided essential guidance for hardware operation, software setup, and interpretation of output data.

- **Numerical Recipes: The Art of Scientific Computing – William H. Press et al.**
  This reference was used to implement numerical techniques for peak detection and curve fitting.

1.3 Problem Statement

The primary objective of this project is to develop a fiber-optic sensing system capable of monitoring an archer's shooting form through data visualized on a custom graphical user interface (GUI). Using a recurve bow as the experimental platform, Fiber Bragg Grating (FBG) sensors are mounted to measure parameters such as strain, vibration, and draw dynamics. These optical sensors are connected to a high-speed interrogator that captures spectral shifts in real-time, enabling detailed feedback for archers.

This project represents a novel integration of optical sensing technology in the context of sports engineering, a field where these methods are not common. To facilitate data acquisition and analysis, the I-MON E High-Speed Interrogator is used in this project. While this commercial interrogator offers a high resolution and reliability, its high cost presents a major barrier to widespread application. This limitation highlights a critical deficiency in current state-of-the-art optical sensing systems.

1.4 Technical Contribution Statement

The team consists of three members with defined roles: Yashil focuses on the mechanical integration of the bow, Metehan focuses on the software side, and I focused on the communication between the optical interrogator and testing as well as the strain measurements. Mechanical components include the physical mounting of two FBGs along the limbs of a recurve bow, as well as fusion splicing. The software components include the programming of an accelerometer and micro-controller as well as a Graphical User Interface (GUI).

My individual contribution to this project was centered around the optical data acquisition and strain measurements. I was responsible for interfacing with the I-MON E interrogator, establishing communication protocols, and configuring its operation to ensure reliable high-speed data capture. This included developing a test bench for the characterization of FBG sensors under various strain conditions to verify their performance and establish a reliable baseline for future experiments.

One of the core tasks I led was the development of MATLAB and Python scripts to extract the Bragg wavelength from each sensor's reflection spectrum. These scripts performed peak detection, spectral fitting, and wavelength shift analysis. Using the standard FBG strain-wavelength conversion relationship which is explored in section 3, the wavelength shifts were then converted into strain values. The extracted strain values, along with the collected and inverted spectra, were then sent to a custom GUI developed by Metehan.

CHAPTER 2

DEVELOPING A OPTICAL BASED ARCHERY TOOL

2.1 Project Objective

The objective of this project is to develop an archery analysis tool capable of capturing and visualizing real-time strain and vibration data through the use of FBG sensors and an Accelerometer. The system aims to provide performance feedback through a graphical user interface (GUI), thereby enabling an archer to evaluate form, draw dynamics, and overall technique.

The system will have Fiber Bragg Grating (FBG) sensors mounted directly onto a recurve bow. These sensors respond to mechanical strain by producing a shift in the Bragg wavelength of the transmitted light. The optical system uses a Superluminescent Diode (SLED) which emits light that travels through the optical fiber and across the FBGs. At each FBG location, a specific wavelength is reflected and the remainder of the spectrum is transmitted. The resulting transmitted signal is routed into the I-MON E High-Speed Spectrum Analyzer. This interrogator converts the received optical signal into an electrical output by mapping the light spectrum across a photodetector array. Internally, the device employs a linear photodiode array and includes a low-noise amplifier (LNA) to boost the electrical signal while minimizing interference. The resulting signal is logged and stored for further processing.

Using the I-MON evaluation software, spectral data is logged and updated in live-time. This data is then exported and processed using custom MATLAB scripts which locate the Bragg peak for each sensor. By comparing the shift in Bragg wavelength relative to an initial baseline, the system calculates the amount of strain experienced at each sensor point along the bow using the relationship between strain and wavelength shift.

In addition to optical strain measurement, the system incorporates an ESP32 microcontroller and an MPU6050 Inertial Measurement Unit (IMU). The MPU6050 provides 3-axis accelerometer and gyroscope data which are used to characterize both the vibrational response of the bow upon release and the orientation of the bow while loaded. The ESP32 handles real-time communication of these motion data, synchronizing them with the optical measurements.

Lastly, the processed data is sent to a Python-based GUI. This GUI enables users to view plots such as Yaw vs time, Acceleration versus time, and Strain versus time. Additionally, the GUI is able to show impulse summary values, such as draw and release data. A flowchart illustrating the objectives of each constituent part is provided below.

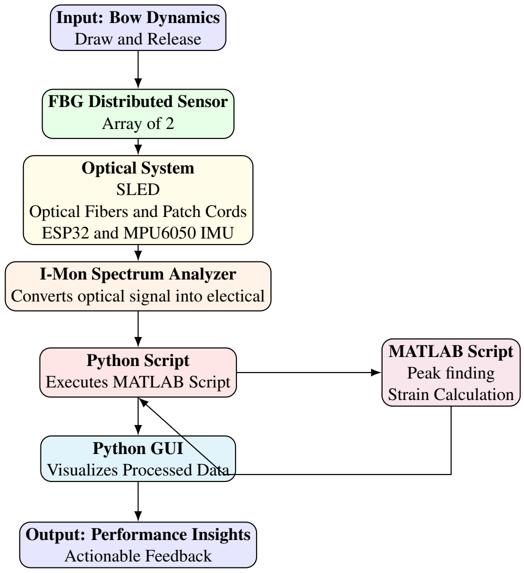

Figure 2.1: Flowchart describing the overall process

2.2 Overall Technical and Engineering Challenges

One of the primary concerns from the beginning of the design process was whether differential strain could be reliably observed along the recurve bow using single-mode optical fibers. Given the localized area of the strain and the relatively small Bragg wavelength shifts associated with fiber deformation, there was initial skepticism regarding whether these shifts would be large enough and distinct to capture meaningful strain differentials. This uncertainty posed a risk to the validity of the measurement system and motivated a careful design of the FBG mounting brackets and interrogation procedures.

In addition to these concerns, several hardware-related failures occurred throughout the year. The most significant of these was the unexpected failure of the laser system used to etch the FBGs. This incident occurred midway through the winter semester and halted our ability to fabricate custom distributed sensors along the same fiber. As a result, we were forced to rely on pre-fabricated loose FBGs, which restricted the sensor layout and prevented us from implementing a 4 array distributed sensor.

The second major issue faced was the malfunction with the I-MON High-Speed Interrogator. The interrogator, which was responsible for acquiring the optical data from the FBGs failed for reasons that remain undetermined.

2.3 Proposed Approach & Solution

The first major challenge addressed was the failure of the laser system used to etch custom Fiber Bragg Grating (FBG) arrays. Originally, the project design involved fabricating a distributed sensor consisting of four evenly spaced FBGs inscribed along a single fiber. This setup would have enabled precise measurements of strain variations at multiple points along the bow. Due to the laser's failure, we were unable to produce this distributed sensor. As a solution, we sourced individual pre-etched FBG sensors from various labs and groups across campus. Ultimately, we were able to acquire eight single FBGs. Given the limitations in supply and the risk of fiber breakage during splicing, we made the decision to fuse two FBGs into a single fiber segment, allowing for partial distributed sensing while maintaining structural integrity. This approach preserved the core functionality of the system by still enabling differential strain measurement, albeit with reduced spatial resolution.

The second major adaptation involved the spectrum analyzer. After the I-MON High Speed Interrogator failed due to an undiagnosed system error, an older generation I-MON interrogator was retrieved and integrated into the system. This older interrogator was operational and compatible with the experimental setup, allowing us to collect spectral data and proceed with testing. However, some communication difficulties emerged during integration with the Python-based graphical user interface (GUI). These issues primarily stemmed from the outdated firmware and network communication protocols of the legacy device, which limited interfacing with the modern Python packages and scripts. Despite this, the system was successfully adapted to enable data collection through the older interrogator and post-processed using MATLAB scripts, meeting the objectives.

2.4 Design Stages

The project was carried out in a series of clearly defined stages, with responsibilities distributed among team members. An outline of the overall design stage with respective responsibilities is provided below.

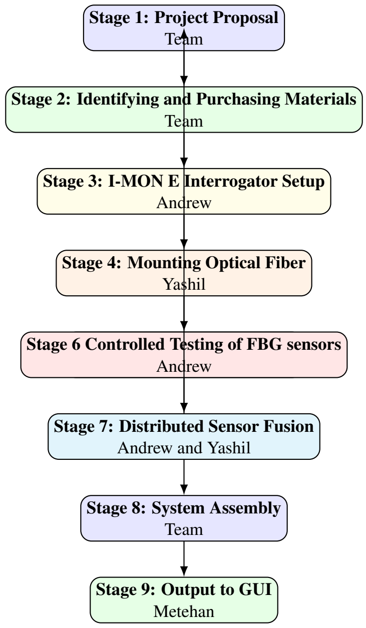

Figure 2.2: Overall Design Process

In Stage 1, the team collaborated to determine the scope and focus of the capstone project. This phase included brainstorming sessions, feasibility analysis, and the proposal preparation. Once the project topic was chosen, Stage 2 involved identifying the required components and hardware. Purchase orders were done by Andrew.

Stage 3 marked the beginning of individual responsibilities. I was responsible for configuring and operating the I-MON E interrogator. This required in-depth calibration, networking setup, and becoming familiar with the spectral acquisition process. In Stage 4, Yashil designed and assembled the optical mounting structure that could safely and securely support bare single-mode fibers along the bow without violating the fiber's minimum bend radius.

In Stage 5, Metehan focused on programming the ESP32 micro-controller and configuring the MPU6050 inertial measurement unit. This allowed us to collect directional and vibrational data from the bow during shooting.

In Stage 6, I conducted controlled testing of individual FBGs using the Fusion test bench. This phase was critical for validating the accuracy of strain measurements and tuning the peak detection algorithm to resolve even small Bragg wavelength shifts as the initial concern was that the peak shift would be negligible.

Stage 7 was a collaborative effort between Yashil and me. We fused two individual FBGs into a distributed sensor unit to replace our original four-sensor design. Despite limited resources, the fusion was successful and the sensor was strong enough to perform in real tests.

In Stage 8, the assembly of the full system took place. This included securing the sensors, ESP32, and IMU in a way that ensured both functionality and safety during dynamic use, connecting to the I-MON E interrogator and the SLED source, and lastly PC.

CHAPTER 3

FIBER BRAGG GRATING THEORY AND STRAIN MEASUREMENT

3.1 Principle

This section focuses on the operating principle behind Fiber Bragg Grating (FBG) sensors and outlines the theory that supports their use in strain measurement applications.

3.1.1 Fiber Bragg Grating Theory

A Fiber Bragg Grating (FBG) is a type of distributed Bragg reflector made within the core of an optical fiber by inducing periodic variations in the refractive index [1]. These periodic structures reflect specific wavelengths of light while transmitting all others. The specific wavelength that is reflected is known as the Bragg wavelength, λ_B, and is given by the fundamental Bragg condition (equation 1) :

$$\lambda_B = 2n_{\text{eff}}\Lambda$$

where n_{eff} is the effective refractive index of the fiber core, and Λ is the grating periodicity [1]. When broadband light is injected into the optical fiber, only the component matching λ_B is reflected, and the remainder of the light is transmitted through the fiber.

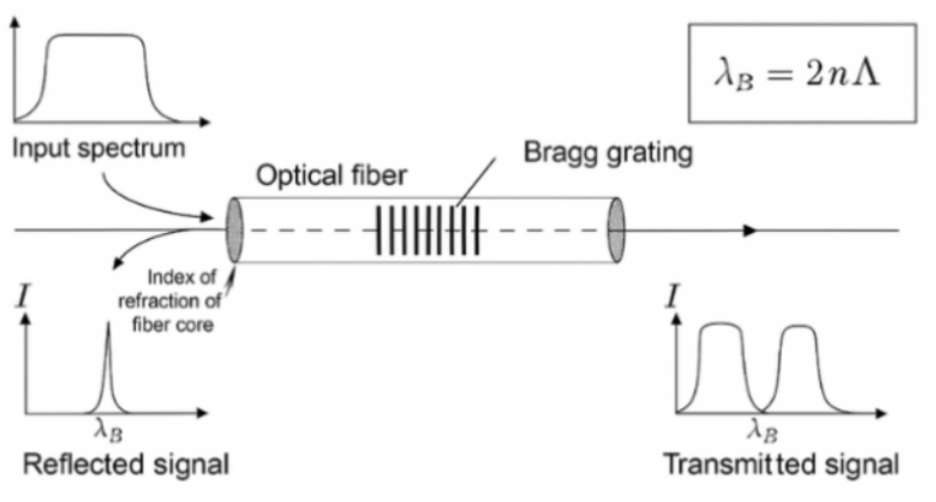

Figure 3.1: Broadband input spectrum with expected transmitted and reflected signals.

As shown in Figure 3.1, the reflected signal consists of a sharp intensity peak at λ_B, while the transmitted signal is a broadband spectrum with a trough or dip at λ_B. The transmitted light appears with a dip due to the removal of the Bragg component from the spectrum.

Strain Response of FBG Sensors

A commonly used model relates the Bragg wavelength shift $\Delta\lambda$ directly to the applied strain ϵ via a gauge factor k, which encapsulates both material and structural properties of the fiber [2]:

$$\epsilon = \frac{\Delta\lambda}{k}$$

Here, k is the **gauge factor**, determined from the manufacturer's specifications . It is a calibration constant that depends on the physical characteristics of the optical fiber and the configuration of the FBG. This method offers a more practical and often more accurate approach in applied sensing scenarios, especially when the optical system has been pre-calibrated which the I-MON E interrogator allows for. It eliminates the need to account explicitly for material constants like the photoelastic coefficient p_e, simplifying the strain calculation [2].

3.1.2 Differential Strain Sensing and Application

In this project, multiple FBG sensors are embedded into the recurve bow in different configurations to capture the localized strain on the bows upper limb. Differential strain sensing is achieved by evaluating the Bragg wavelength shifts from two FBGs placed at symmetric locations on the bow. This configuration allows for detection of asymmetry in form or force, which is valuable in archery coaching and feedback applications.

By tracking the wavelength shift from each sensor, and comparing them, the system can identify variations in draw strength or imbalances between limbs of the archer. This differential analysis provides higher resolution insight into shooting technique, body posture, and shot consistency.

3.2 Technical Challenges

Several technical challenges arose throughout the development and integration of the sensing and data acquisition system. These challenges were addressed in the context of literature on fiber optic sensing and signal processing but also required experimental adaptation due to the project objectives.

- **I-MON Interrogator Replacement and Communication Issues:**
  Midway through the project, the original I-MON High-Speed Interrogator failed due to an undiagnosed system error. To continue development, we replaced it with an older generation I-MON interrogator. Although this backup unit functioned well for data acquisition, its outdated firmware created communication conflicts with our Python-based data pipeline. Specifically, the UDP socket communication protocol used by the Python GUI was not fully compatible with the legacy device's internal buffer structure. This incompatibility introduced timing issues and forced us to implement workaround routines in the script to reliably extract raw data and relay it to MATLAB.

- **Optical Fiber Routing and Signal Integrity:**
  One of the earliest technical concerns involved the physical layout of the optical fibers. Due to the sensitivity of single-mode fibers, they had to be mounted along the recurve bow in a manner that avoided excessive bending, power saturation, or signal loss. According to established guidelines, the fibers were not allowed to exceed a minimum bend radius of approximately 4 cm. Despite this precaution, we encountered issues with signal attenuation and inconsistent responses in some trials, likely due to bends introduced during mounting. These issues were addressed and tested using the test bench to determine which mount allowed for signal transmission with minimal loss. The final mounts designed by Yashil were able to hold the bare fiber with minimal loss and meet the project objectives. An image of the testing process is provided below in figure 3.2.

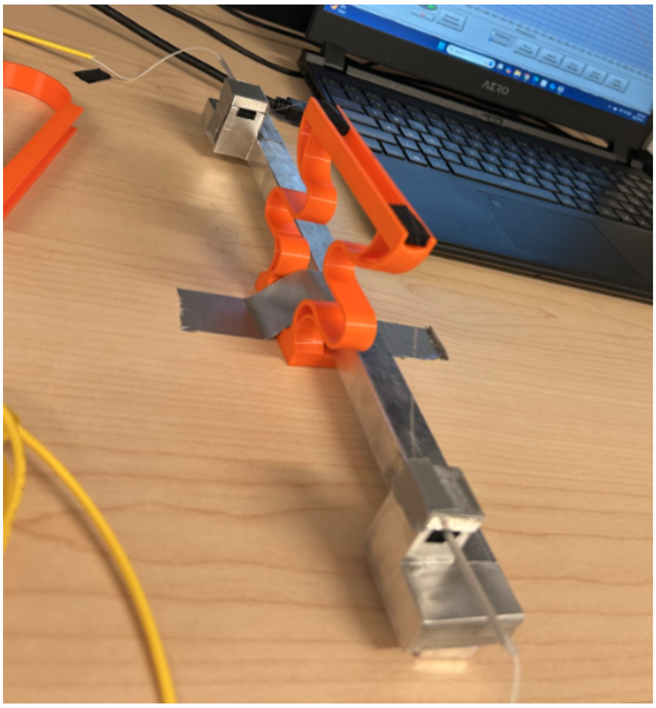

Figure 3.2: Fusion Demo Bench using old mount to determine amount of loss with bending.

- **MATLAB Peak Detection and Bragg Wavelength Extraction:**
Another challenge emerged in developing a MATLAB script that could accurately detect the Bragg wavelength from the transmitted signal. Unlike reflected spectra, which present a distinct peak at the Bragg wavelength, the transmitted signal manifests as a trough at that same location. This inversion required modifying the peak detection algorithm to identify local minima rather than maxima. An image of the transmitted signal is provided below in figure 3.3

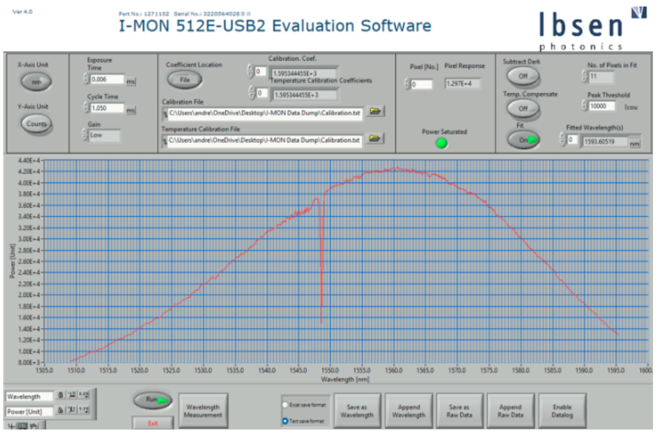

Figure 3.3: LabVIEW Evaluation Software displaying the transmitted signal with a singular FBG.

3.3 Important Design Aspects: Features & Limitations

The sensing and feedback system developed for this project integrates optical sensing, embedded electronics, and real-time signal processing. Several important features make the system well-suited for performance tracking in archery, but there are also design limitations. The key features and limitations are discussed below.

Key Design Features

- **High Sensitivity and Precision:**
The use of Fiber Bragg Grating (FBG) sensors combined with the I-MON E interrogator enables the

system to detect microstrain level variations in the optical fiber. The interrogator offers a wavelength resolution up to 1 pm and a sampling rate of up to 2 kHz, which provides excellent sensitivity for monitoring small mechanical deformations during the archer's draw and release.

- **Real-Time Feedback with Minimal Latency:**
  A major strength of the system is its ability to process and visualize data in real-time. The I-MON continuously logs the optical spectrum as an intensity vs. wavelength array, which is then parsed by a MATLAB script. This script detects the spectral peaks by comparing the newly logged file to the previous data and updates the peak plots accordingly. By overwriting old values with new data and extracting Bragg peak positions in a looped routine, the Matlab script can track spectral shifts almost instantly. Both the reflected and transmitted FBG spectra are visualized with minimal delay, which is essential for athletic applications where dynamic feedback is crucial.

- **Portability:**
  The use of the I-MON E interrogator significantly increases the system's portability. Its compact form factor and external USB/Ethernet interface allow the setup to be moved easily from the lab to the field without requiring a complex hardware infrastructure. This contrasts with bench-top spectrometers or fiber-coupled lab interrogators, which are typically bulky and sensitive to vibration.

Design Limitations

- **Temperature Dependency:**
  Like all FBG-based sensing systems, the Bragg wavelength is not only sensitive to strain but also to temperature fluctuations. However, in this project, the operating environment was assumed to be thermally stable, and temperature variations were considered negligible.

- **Limited Scalability:**
  The current implementation is specialized for a recurve bow and is not generalized for broader athletic use without modification. However, the modular nature of the system components (the FBG sensors, I-MON interrogator, ESP32 microcontroller, and MPU6050 IMU) makes it adaptable to other sports equipment. With adjusted mounting techniques and calibration, the same sensing methodology could be extended to tennis rackets, baseball bats, or golf clubs

- **Limited Real-Time FFT Analysis:**
  One of the limitations introduced by switching from the I-MON 256 High-Speed to the I-MON 512 E interrogator was the loss of real-time Fast Fourier Transform (FFT) capability. The I-MON 256 included internal firmware and a buffer management system that allowed for high-rate streaming. In contrast, the I-MON E model relies on longer acquisition-to-write delays and reduced memory buffer access, which hinders the use of live FFT operations. As a result, vibrational frequency content could not be processed in real time through the use of FBG but was through the use of a MPU6050

3.4 Comparison with State-of-the-art techniques

Despite being an older-generation device, the I-MON E interrogator remains a capable and precise optical interrogation system. It enables high-resolution, real-time spectral acquisition of Fiber Bragg Grating (FBG) signals, which is essential for capturing dynamic strain responses in a recurve bow.

Signal analysis in this project was performed using MATLAB, where a peak-tracking algorithm was implemented to extract Bragg wavelength shifts from acquired data. This approach provided flexibility in algorithm design and data visualization. Compared to more common vendor-based solutions, which often rely on LabVIEW, MATLAB offered greater transparency and adaptability.

The method of calculating strain from FBG data in this system is based on the shift in Bragg wavelength, using the empirical relationship:

$$\epsilon = \frac{\Delta\lambda}{k}$$

where $\Delta\lambda$ is the wavelength shift and k is the calibrated gauge factor for the fiber. This approach provides direct strain measurements with high sensitivity and immunity to electromagnetic interference, making it ideal for integration into composite or flexible structures such as archery equipment.

In contrast, traditional strain measurement techniques for bows or similar mechanical systems often utilize electrical resistance strain gauges. These sensors measure strain by detecting changes in electrical resistance as the material deforms. While strain gauges are compact and inexpensive, they are highly susceptible to electrical noise, temperature drift, and mechanical fatigue over time. Additionally, their data is typically acquired as voltage signals and requires analog-to-digital conversion and calibration against baseline resistance values, introducing more sources of error.

Compared to these methods, FBG-based sensing offers superior resolution, multiplexing capability, and immunity to environmental noise. Although optical interrogation systems such as the I-MON E are more complex to set up and expensive, the overall accuracy, precision and long-term stability make FBGs a compelling alternative for precision strain analysis in sports engineering applications.

3.5 Alternative Techniques

Alternative approaches were explored for their potential to accomplish data collection and analysis. While these strategies offered different advantages, they were omitted due to specific limits and challenges linked to the data processing and strain analysis component. This section explains the alternatives and provides arguments for their exclusion.

Direct Machine Learning Models

Machine learning (ML) techniques were explored to analyze strain data and extract performance metrics dynamically. By training models on sensor data, ML could identify patterns and predict performance metrics. This idea was abandoned due to complexity and time-line considerations. **Advantages:**

- Dynamically adapts to non-linear relationships between wavelength shifts, strain, and tension.

Reasons for Exclusion:

- Introduces system complexity, necessitating significant computational resources and expertise.
- Increases latency, making it incompatible with the need for real-time feedback during bow operation.

Real-Time Python-Only Processing

A Python-only processing framework using libraries such as NumPy or Pandas could replace the MATLAB analysis. This approach eliminates MATLAB dependency while maintaining core processing capabilities. **Advantages:**

- Simplifies system design by reducing reliance on proprietary software.
- Cost-efficient due to Python's open-source nature.

Reasons for Exclusion:

- MATLAB provides visualization and data analysis features that are challenging to replicate in Python.
- Transitioning to Python would require re-implementing MATLAB algorithms, greatly increasing development time.

Alternative to I-MON E Interrogator

As an alternative to the expensive I-MON E interrogator provided by Ibsen Photonics, an affordable optical interrogator is explored in the flow chart provided below. **Advantages:**

- Allows for remote monitoring and processing, enabling users to use the device wherever they desire.
- Significantly reduces costs and opens the possibility of commercializing the product.

Reasons for Exclusion:

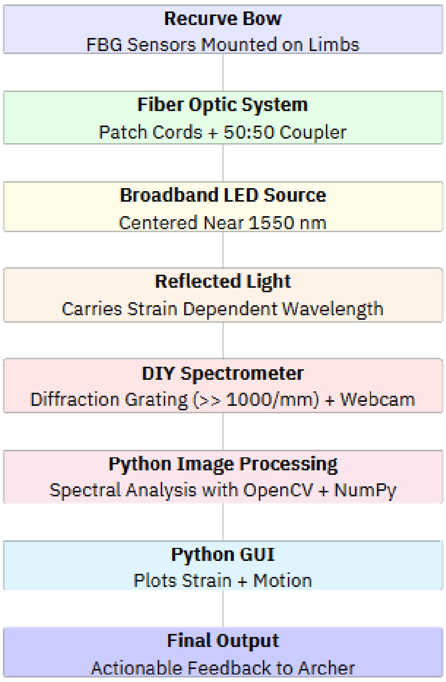

Figure 3.4: Alternative optical interrogator proposal to replace I-MON E

- Able to obtain an older Ibsen interrogator.
- Required additional funding.
- Significantly reduced speeds and resolution when compared to the high speed models.

CHAPTER 4

EXPERIMENTAL DEMONSTRATION

4.1 Design Considerations

Sensor Placement and Mounting Strategy

Due to the bow's curvature and flexibility, mounting the optical fiber required a solution that would not interfere with normal bow operation while maintaining consistent strain transfer. The selected approach used custom 3D-printed fiber compressors and spring-loaded clips to secure the SMF-28 fiber directly along the limb of the bow. These mounts ensured stable contact and reduced the risk of slippage or decoupling during high-speed limb movement. The central grip area was intentionally left fiber-free to maintain archer comfort and form integrity.

Interrogator and Sensor Compatibility

The I-MON E interrogator was selected for its ability to provide high-speed spectral acquisition with a wavelength resolution below 1 pm. Despite being an older-generation device, its 512-pixel detector and real-time USB 2.0 streaming interface made it suitable for capturing strain measurements.

Algorithm Design and Data Processing

Given the short duration and high-frequency characteristics of the strain event, an efficient peak detection method was required. MATLAB was selected due due to its flexibility in algorithm development, its compatibility with I-MON data structures, and its powerful visualization tools.

Strain Calibration Methodology

The strain computation method is a simplified gauge-factor approach that was explained in section 3.1:

$$\epsilon = \frac{\Delta\lambda}{k}$$

A custom test bench was designed to facilitate this calibration, ensuring that the calculated strain values closely reflected actual mechanical loads applied to the fiber.

System and Repeatability

Durability of the fiber mounting system was also considered to ensure repeatability across multiple test shots. All fiber routing and anchoring mechanisms were designed to minimize movement and bending losses.

4.2 Design Implementation

Mechanical Integration

The bow limbs were equipped with a custom mounting system consisting of 3D-printed fiber compressors and spring-loaded holders. These components secured the SMF-28 optical fiber directly to the surface of the bow, ensuring consistent mechanical coupling while avoiding damage to the fiber. A total of six mounting points were installed along each limb: three to compress the fiber into place along the right side and three along the left. The design allowed the optical fiber to experience strain corresponding to the bow's flexing under draw and release and monitor the differential strain.

An additional central mount was used to secure an ESP32 micro-controller and an MPU-6050 inertial measurement unit (IMU). An image of the product used in the demonstration with major elements highlighted is provided below by figure 4.1.

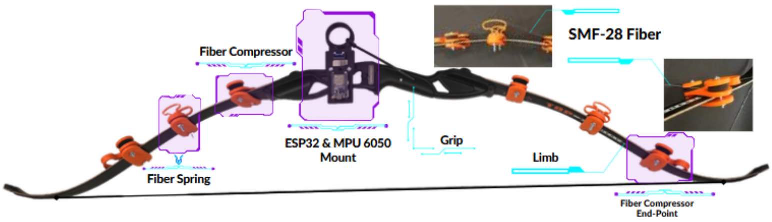

Figure 4.1: Final product design with major elements outlined. [Yashil]

Optical and Interrogation System

The light source in this project is a Superluminescent LED (SLED), transmitting light through a single-mode SMF-28 fiber containing FBG sensors. These FBGs were strategically written to reflect specific wavelengths that shift under strain. The reflected spectrum was captured using an Ibsen Photonics I-MON E interrogator.

Although the I-MON E is an older device, it provides high spectral resolution and real-time acquisition capabilities comparable to modern systems. It features a 512-pixel linear array with a wavelength range of 1510-1595 nm and a maximum sampling rate of 2 kHz. These specifications enabled accurate tracking of wavelength shifts during rapid dynamic loading events, such as the release of an arrow.

Signal Processing and Strain Calculation

The I-MON E interrogator transmits raw spectral data to a PC via USB 2.0. A custom MATLAB script was developed to process this data. The script applies Gaussian smoothing and interpolation to the intensity spectrum, followed by a peak-finding algorithm to extract the reflected Bragg wavelength from each FBG.

The strain, ϵ, was then computed using the relation:

$$\epsilon = \frac{\Delta\lambda}{k}$$

where $\Delta\lambda$ is the shift in reflected wavelength and k is the gauge factor specific to the fiber and mounting configuration [1]. The use of a calibrated gauge factor simplified computation and eliminated the need to account for the photoelastic coefficient.

Test Bench and Calibration

A test bench was designed and fabricated in a machine shop to measure FBG sensors and their responses. This setup allowed calibration of the gauge factor k by measuring wavelength shifts This calibration data was used to validate the accuracy of strain measurements in the full bow-mounted system.

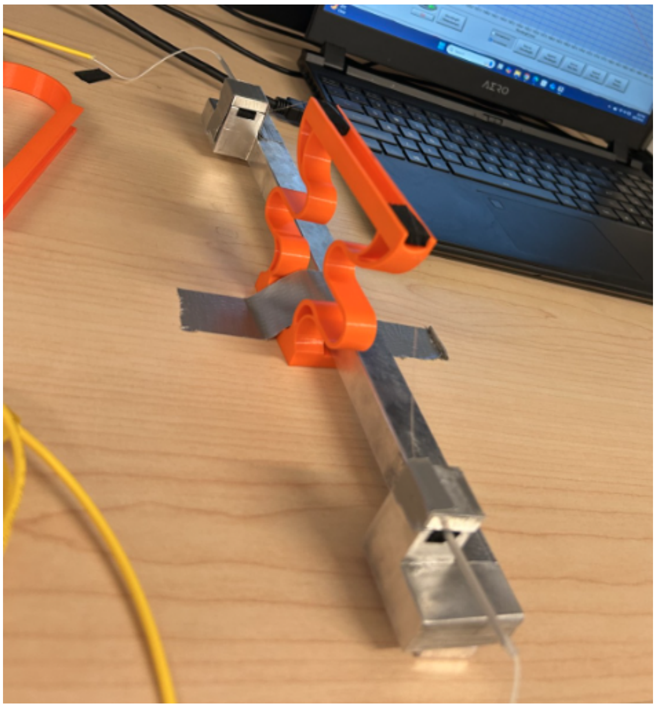

Figure 4.2: FBG test bench, designed for bare fiber placement.

Data Visualization and Future Expansion

The MATLAB interface included real-time plotting of spectral peaks and strain values. The system architecture was designed with modularity in mind, allowing expansion to support multiple FBGs.

4.3 Hardware Setup

4.3.1 Optical Fiber Mounting System (Yashil)

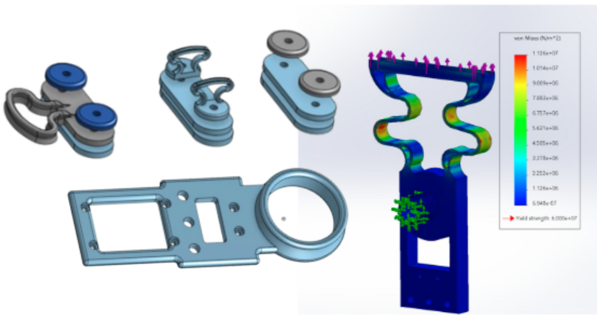

Figure 4.3: SMF-28 and FBG Mounting System (Yashil Thakore)

The mount design process for the Fiber Bragg Grating (FBG) sensors on the archery bow was an iterative process. Designing the mount involved two key constraints:

- Ensuring a sufficient radius of curvature for the fiber cables to avoid signal loss
- Applying just enough tension to detect Bragg wavelength shifts without exerting force on the limbs, and preserving the limbs' natural flexibility.

The springs were designed after gaining an understanding of the force distribution in the CAD tool.

Materials and Methods

The mounts were printed with mostly TPU as it's flexible and soft enough to allow the fiber to maintain tension during use. The fiber was compressed at 2 points between 2 gripper pads (meant to prevent slippage). The middle portion acts as a spring to allow the fiber dynamic movement. The sensor rests in-between the spring, and the tensioned point such that strain can be measured. Finally, the ESP32 and MPU6050 are mounted on the center mount.

4.3.2 I-MON E Interrogator 512 (Andrew)

Figure 4.4: Ibsen Photonics I-MON E Interrogator 512

The I-MON E-USB 2.0 interrogator was responsible for acquiring spectral data from the Fiber Bragg Grating (FBG) sensors embedded in the recurve bow. The I-MON interrogator converts the raw optical signal that passes through the FBGs into a plot of intensity (counts) versus wavelength (nm).

Light entering the device is dispersed across the sensor array using a diffraction grating. That array has 512 pixels, allowing for high-resolution spectral readings, with shorter wavelengths directed toward higher pixel indices and longer wavelengths captured at lower pixel positions. The result is a spatially resolved spectrum, which the I-MON software presents as intensity (counts) versus wavelength (nm).

The key specifications of the I-MON E used in this project are as follows:

- **Wavelength Range:** 1510 nm to 1595 nm
- **Spectral Resolution:** Approximately 1 pm
- **Pixel Count:** 512 pixels
- **Sample Rate:** Up to 2 kHz
- **Dynamic Range:** Up to 55000 counts (before power saturation occurs)
- **Output Format:** Intensity (counts) vs. Wavelength (nm)

During testing, the interrogator was connected to a PC via USB 2.0 and operated using the I-MON Evaluation Software. This software was configured to log spectral data in real time. The data was saved in raw formats and transferred to MATLAB for analysis. The X-axis of the output data was calibrated in nanometers using a 5th-degree polynomial based on EEPROM-stored coefficients, while the Y-axis provided intensity in counts.

Figure 4.5: Ibsen Photonics Superluminescent LED Source (SLED)

Following the acquisition, MATLAB scripts processed the I-MON data to identify peak wavelength positions. These values were continuously updated in a logging loop that compared each new spectrum to the previous frame. Strain was calculated by observing the shift in the Bragg peak over time and was then visualized in a GUI alongside accelerometer and orientation data from the ESP32 and MPU6050 components mounted on the bow.

4.3.3 Denselight Superluminescent Diode (Andrew)

To illuminate the Fiber Bragg Gratings (FBGs), a broadband optical source was used. This project uses a DL-BP1-1501A Superluminescent LED (SLED).

The DL-BP1-1501A model integrates an optical circulator and is designed for single-mode fiber output. The light source emits a broadband spectrum centered around 1550 nm, with a spectral bandwidth greater than 40 nm. This broad output is essential for FBG sensing, where each sensor reflects a narrow band within the source's emission range.

The optical setup begins at the SLED's FC/APC source, from which the broadband light is coupled into the fiber. After passing through the FBG array, the remaining transmitted spectrum is collected by the I-MON E interrogator for processing. The SLED also provides a RETURN port on its circulator for optional reflected signal measurements.

Key specifications of the DL-BP1-1501A are as follows:

- **Central Wavelength:** 1550 nm
- **Spectral Bandwidth:** >40 nm
- **Optical Output Power:** Up to 2.5 mW (in CW mode, ACC control)
- **Output Interface:** FC/APC Single-Mode Fiber
- **Modulation Modes:** CW, internal modulation (1–10,000 Hz), external modulation via SMA
- **Power Supply:** +5 VDC via 4-pin terminal block
- **Control Interface:** USB Mini-B with GUI software

The SLED supports three operating modes: CW (continuous wave), internal modulation, and external modulation. In this project, CW mode was used under Automatic Current Control (ACC) conditions. The device was powered through a +5 VDC supply and controlled via the USB interface using the included GUI application BP1Interface. This allowed direct control over output power and modulation settings.

The use of the DL-BP1-1501A ensured stable, broadband optical power for the FBG interrogation system and was critical in achieving the necessary wavelength coverage and resolution for strain sensing across the mounted sensor array.

4.3.4 MPU6050 6-axis Motion Tracking Device (Metehan Kocaman)

A MPU6050 Inertial Measurement Unit (IMU) was integrated into the system to provide real-time motion and orientation data. The MPU6050 combines a 3-axis gyroscope and a 3-axis accelerometer on a single chip, allowing it to simultaneously track both angular velocity and linear acceleration. The device was mounted near the grip of the bow to ensure it captured the most relevant physical dynamics during each shot.

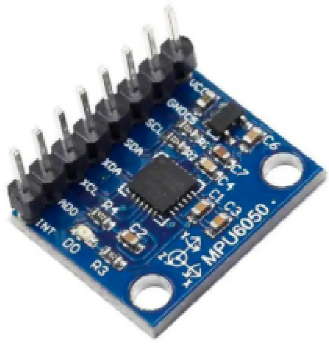

Figure 4.6: MPU6050, 6-axis motion tracking device.

Data from the MPU6050 was sent to a microcontroller unit (ESP32), which parsed the sensor readings and relayed them to the Python GUI for visualization. Two key features enabled by the IMU are:

- **Yaw (Gyro Z):** Measures the rotational twist of the archer's hand around the vertical axis of the bow. This provides insights into postural consistency and unintended torque during release.
- **Acceleration Magnitude:** Computes the magnitude of the 3-axis acceleration vector to represent the total vibrational impulse imparted on the bow upon arrow release.

These signals were plotted in the GUI alongside the optical strain data to provide visualization of the mechanics behind a shot. For each shot, the following values were stored:

- Yaw angle (Z-axis gyroscope) versus time
- Acceleration magnitude versus time
- Impulse summary values (duration, peak strain, max acceleration)

All data streams, including strain, yaw, and acceleration, could be saved from the GUI as .CSV files for further offline analysis. The inclusion of the MPU6050 enhances the multi-modal sensing capability of the system and provides valuable biomechanical context to the FBG-based strain measurements.

4.3.5 ESP32 Microcontroller (Metehan Kocaman)

The ESP32 micro-controller was used as the embedded processing platform. In this project, the ESP32 served three main functions:

- **Sensor Communication:** The ESP32 interfaced with the MPU6050 to retrieve gyroscope and accelerometer data.
- **Real-Time Data Parsing and Transmission:** The collected IMU data was preprocessed to calculate relevant features such as yaw angle and acceleration magnitude.
- **Integration with Python GUI:** The ESP32 continuously sent formatted data packets to the Python-based GUI, which parsed the incoming data for real-time plotting and statistical analysis. Features such as strain vs. time, yaw tracking, and acceleration impulse were rendered in real time for each recorded shot.

The ESP32 was powered via USB and programmed using the Arduino IDE, using the Wire and MPU6050 libraries for sensor communication and serial handling. Its compact size allowed it to be mounted directly on the bow near the MPU6050 without interfering with shooting.

Figure 4.7: ESP-32 Microcontroller

4.4 Measurement Results

4.4.1 FBG Peak Finding

Data was taken to verify the performance of the distributed Fiber Bragg Grating (FBG) sensor array and validate the accuracy of the MATLAB peak detection algorithm. The optical fiber used in this test contained two FBGs, originally inscribed to reflect at center wavelengths of 1534 nm and 1543 nm.

Figure 4.8 presents the residual spectrum captured by the I-MON E interrogator for the dual-FBG setup. Overlaid on the residual plot are the identified peak locations, extracted using a custom MATLAB script that applies Gaussian smoothing, threshold filtering, and a local maximum-finding algorithm to detect Bragg reflections.

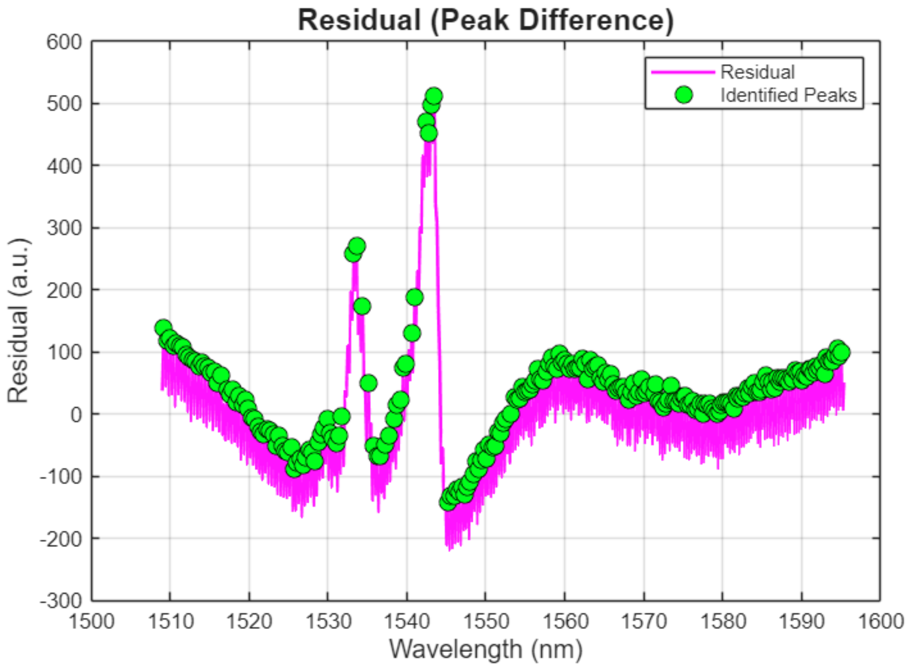

Figure 4.8: FBG reflection spectrum for distrubuted sensor with array of 2 FBG (Data from demonstration)

From the spectrum and corresponding residual analysis, the following peaks were identified:

- **1531.2 nm**, corresponding to the FBG mounted on the right side of the upper limb, with a peak residual amplitude of 269.98 a.u.
- **1540.5 nm**, corresponding to the FBG mounted on the left limb, with a peak residual amplitude of 512.85 a.u.

These measured wavelengths deviate from their expected values of 1534 nm and 1543 nm by 2.8 nm and 2.5 nm, respectively. The observed asymmetry could be from the loading between limbs. Specifically, the larger shift observed on the left of the top limb (peak to the right) may be a result of improper wrist positioning or inconsistent draw technique, causing uneven distribution of mechanical stress during the shot cycle.

This interpretation aligns with the physical configuration of the bow during testing, where slight hand misalignment could result in differential strain between the limbs. The sensitivity of the FBG system to such variations highlights its potential as a tool for technique refinement in archery. Additionally, the accurate detection of asymmetric strain confirms the effectiveness of the MATLAB peak detection algorithm and validates the reliability of the optical signal acquired through the I-MON E interrogator.

4.4.2 Strain Measurement

Following the successful detection of the Bragg peaks and noticing a differential shift, the next step was to compute the mechanical strain experienced by each FBG sensor. Strain was derived directly from the shift in Bragg wavelength using the linear relation [1]:

$$\varepsilon = \frac{\Delta\lambda}{k}$$

where ε is the strain, $\Delta\lambda$ is the change in Bragg wavelength, and k is a proportionality constant related to the strain sensitivity of the fiber [1]. The value used in this project is: $k = 1.2 \times 10^{-3}$ nm$/\mu\varepsilon$.

The unstrained (rest) Bragg wavelengths were 1543 nm and 1534 nm, respectively. After loading the bow, these peaks shifted to 1540.5 nm and 1531.2 nm. Using the strain equation:

$$\varepsilon_{\text{right}} = \frac{1540.5 - 1543}{1.2 \times 10^{-3}} = -2088.7\ \mu\varepsilon$$
$$\varepsilon_{\text{left}} = \frac{1531.2 - 1534}{1.2 \times 10^{-3}} = -2033\ \mu\varepsilon$$

The negative values indicate compressive strain on both sensors, as the Bragg wavelengths decreased. Importantly, the strain magnitudes differ: the left side of the bow experiences approximately 55.6 $\mu\varepsilon$ more compression than the right side. This asymmetry suggests that the archer's draw was not perfectly balanced, applying slightly more force to one limb. This result validates one of the primary motivations for the project: detecting differential strain.

4.4.3 Final GUI (Metehan)

To assist with the post-processing and visualization of experimental data, a custom graphical user interface (GUI) was developed in Python. The GUI provides a synchronized display of strain, yaw, and acceleration magnitude

As illustrated in Figure 4.9, the user interface allows archers or evaluators to analyze bow performance following each arrow release. The interface displays three real-time plots:

- **Acceleration Magnitude:** Derived from the 3-axis accelerometer on the MPU6050. This plot reveals the vibrational response of the bow after release and helps characterize impulse and shock dynamics.

- **Yaw (Gyro Z):** Reflects rotational twist around the vertical axis, quantifying hand stability and postural drift during the shot.

- **Strain vs. Time:** Displays the strain values derived from Bragg wavelength shifts provided via MATLAB.

The interface also provides a 3D orientation plot of the bow's real-time position, reconstructed using the raw gyroscope data. All time-domain data streams are synchronized and plotted against a common timeline for comparative analysis. A CSV export option allows users to save shot data for deeper offline examination or performance tracking over time.

Additional features include a stats panel that displays shot duration, peak strain, maximum acceleration, and strain impulse. These summary statistics allow for side-by-side comparisons of successive shots and can highlight inconsistencies in draw force or posture.

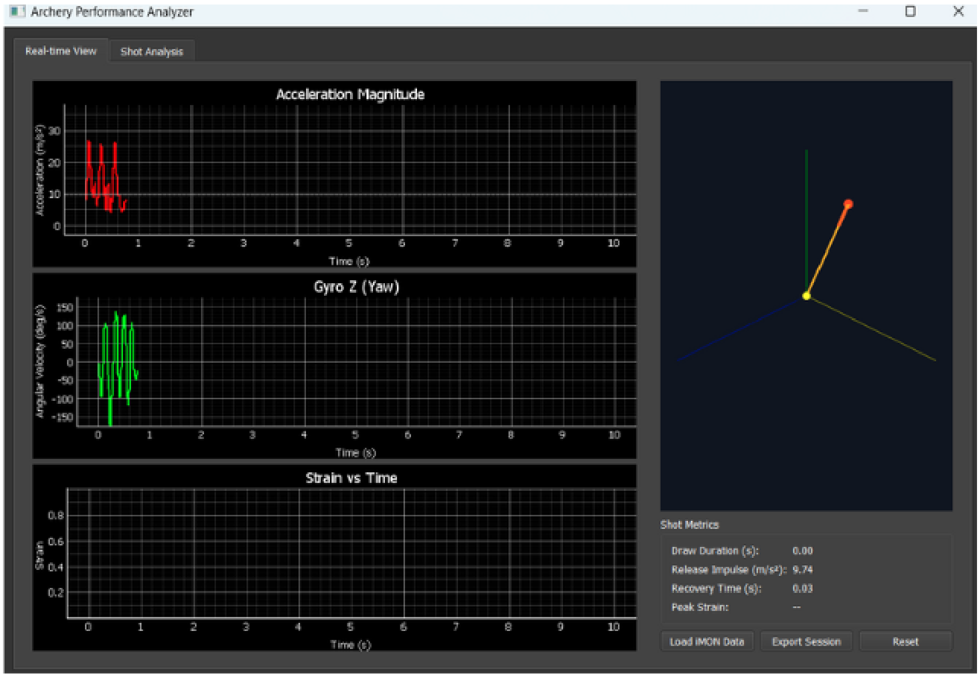

Figure 4.9: Final Graphical User Interface without the Strain Measurement. (Metehan Kocaman)

4.5 Discussions

The primary objective of this project was to detect differential strain between two Fiber Bragg Grating (FBG) sensors embedded on the limbs of a recurve bow. Despite setbacks related to hardware failures, the system successfully demonstrated its ability to measure and distinguish strain magnitudes across both limbs. The results revealed that:

- The **right-side** FBG sensor experienced a wavelength shift from 1543 nm to 1540.5 nm, corresponding to a strain of approximately $-2088.7\ \mu\varepsilon$.
- The **left-side** FBG sensor shifted from 1534 nm to 1531.2 nm, corresponding to $-2033.1\ \mu\varepsilon$.

The unit of measurement, microstrain ($\mu\varepsilon$), represents strain on the order of one part per million. A difference of 55.6 $\mu\varepsilon$ between the two limbs suggests a small but measurable imbalance in the archer's form, validating the system's potential for use in coaching. The strain values align with expected magnitudes for the draw and release forces involved in archery and confirm that the Bragg wavelength shifts can be interpreted reliably using the developed MATLAB analysis pipeline.

However, one of the most significant deficiencies in the system was the inability to achieve real-time strain visualization. This limitation was primarily due to a critical hardware failure that occurred in March, when the original I-MON 256 High-Speed interrogator stopped functioning. The replacement I-MON E modern communication support and had trouble exporting data in formats compatible with the real-time MATLAB processing routines. As a result, all strain analysis had to be performed in post-processing, reducing the immediate feedback potential of the system during live testing sessions.

Despite this limitation, the embedded motion sensing subsystem, consisting of the MPU6050 inertial measurement unit and ESP32 micro-controller, performed exceptionally well. The accelerometer accurately captured the vibrational response of the bow during and after release, while the gyroscope successfully recorded rotational twist, offering insights into hand posture stability. Additionally, the real-time yaw tracking and orientation visualization allowed for consistent directional analysis of the bow, contributing meaningful feedback.

In conclusion, while the core functionality of strain measurement was achieved confirming the objective, the lack live-time data analysis limited the system's functionality. The performance of the motion subsystem was successful in delivering a fully integrated, real-time feedback for archery performance monitoring.

CHAPTER 5

CONCLUSIONS

5.1 Summary

This project successfully demonstrated the feasibility of using FBG sensors in combination with an IMU to monitor key aspects of archery performance. The final prototype was capable of tracking directional orientation, postural hand twist, shot duration, and vibrational impulse. The graphical user interface (GUI) provided real-time visualization of acceleration magnitude, yaw (Gyro Z), and Bragg wavelength peak shifts.

Although live-time strain computation was not achieved due to hardware limitations and lack of time, specifically the failure of the I-MON 256 High-Speed interrogator and the restricted capabilities of the replacement I-MON E unit, the project still succeeded in proving the initial concept of measuring differential strain.. The recorded Bragg peak shifts were used in post-processing to calculate strain, revealing a measurable difference between the left and right FBG sensors. This strain asymmetry provides evidence of postural imbalance during the archer's draw, meeting the central goal of the system.

5.2 Overall Project Contributions and Achievements

My primary contributions to the capstone project were focused on the development, operation, and troubleshooting of the optical interrogation system, specifically the I-MON interrogators and the strain measurement system based on Fiber Bragg Grating (FBG) sensors.

I-MON E Interrogator Operation

A significant portion of this project involved the integration and operation of optical interrogation hardware used to capture Bragg wavelength shifts from Fiber Bragg Grating (FBG) sensors. One of my primary contributions was centered around the setup and configuration of the I-MON 256 High-Speed interrogator. This device was designed for high-frequency optical data acquisition and presented a opportunity to test real-time strain sensing within the archery application.

A major portion of time from Janurary to early March was spent working on the communication with the I-MON 256 High Speed interrogator The I-MON 256 High-Speed unit communicated via a combination of UDP and TCP protocols over Ethernet, with control commands issued through Telnet and data packets transmitted using a specific binary UDP format. The initial configuration involved IP address management, port forwarding, and the use of diagnostic tools such as PuTTY, Wireshark, and Nmap to establish and monitor communication with the interrogator. Extensive effort was invested into aligning the system IP with the device's expected subnet range and ensuring that the necessary communication ports were not blocked by local firewall rules or administrative network settings.

Despite configuring the system in alignment with the manufacturer's documentation, the interrogator continuously returned communication errors such as "Error -22, failed to establish Telnet connection". This issue proved difficult to isolate due to a lack of debugging documentation and limited manufacturer support. Over multiple weeks, the configuration was tested across different operating systems, Ethernet adapters, and router setups. Custom scripts were even written to simulate client-server socket handshakes in both TCP and UDP modes to verify the device's response state. Unfortunately, the I-MON 256 continued to resist stable communication, making it unusable.

It became clear that resolving the issue required a deeper understanding of low-level network socket programming and proprietary firmware behavior. After discussing the issue with the team and consulting with support channels, an alternative interrogator was obtained: the I-MON USB E, a more user-friendly variant that interfaces with a PC through a USB 2.0 connection. This change significantly reduced setup complexity, as the USB interface required no networking configuration, and the device could be directly accessed using manufacturer-supplied DLLs and drivers. Transitioning to the I-MON E enabled successful implementation of the data acquisition system and allowed the focus to shift toward MATLAB-based data processing.

FBG Strain Measurement and Peak Tracking

Using the optical interrogators, I developed and verified a MATLAB script capable of identifying Bragg wavelength peaks in real-time. This script continuously read spectral data from a CSV log file generated by the I-MON software, applied smoothing and peak-detection filters, and plotted the evolving peak positions. The shift in Bragg wavelength was converted to strain using the linear relation $\varepsilon = \Delta\lambda / k$.

After the original interrogator suffered a critical failure in March, we replaced it with an older I-MON E model. However, the new device introduced unforeseen limitations. Most critically, it failed to export standard CSV files. Despite the ".csv" extension, the files generated by the I-MON E software were incorrectly encoded or formatted, causing MATLAB to misinterpret them as non-text files (e.g., UTF-16 encoded or malformed headers), rendering the script unable to work in live time. Due to this issue, I transitioned to static, post-shot data analysis to confirm differential strain.

FBG Test Bench Design and Fabrication

Another key contribution was the design and construction of an FBG test bench used to validate our sensing methods prior to full system integration. The test bench was designed in Fusion 360 and manufactured at the machine shop using 6060-grade aluminum. It consisted of two adjustable clamps with soft rubber padding capable of gently holding bare optical fibers without inducing microbending or signal loss. This setup was essential for evaluating the fibers' sensitivity to strain and mechanical deformation before mounting them to the bow.

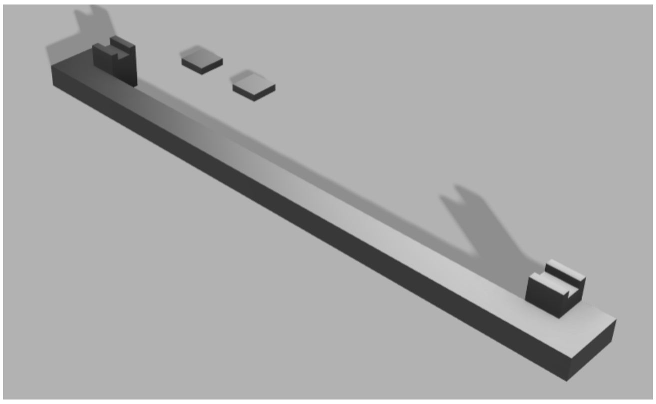

Figure 5.1: Fusion test bench deisgned for bare optical fibers.

Using this test bench, I conducted controlled experiments to examine the effects of fiber bending on optical signal integrity. One successful trial involved bending a fiber with a single FBG to a radius of 5 cm while monitoring reflected intensity and wavelength. The experiment demonstrated that as the bend radius decreased, the signal intensity also dropped, due to mode mismatch and scattering losses. Notably and as expected, no significant Bragg wavelength shift was detected during the bending alone, confirming that bending primarily affected signal power rather than strain-induced wavelength shifts. This data informed the minimum bend radius constraints used in final mount design.

Purchase Orders

In addition to technical development, I was responsible for submitting and tracking purchase orders throughout the year. The items included included: optical fibers, patch cords, sleeve protectors, and the Recurve bow.

Significance and Impact of Contributions

The successful measurement of differential strain was a central objective of this capstone project. My work ensured that the system could detect subtle differences in strain between the two limbs of the recurve-bow data which directly reflects an archer's posture, technique, and draw symmetry. For instance, the final static measurements showed that the left-side FBG experienced approximately 55.6 $\mu\varepsilon$ more compression than the right-side FBG, indicating a small imbalance in form. Without the peak-tracking scripts, test bench experiments, and FBG validation procedures. The entire method would remain in question. Testing of individual sensors allowed for a quick transition to the next stage of assembling the recurve-bow apparatus for measurements.

Despite hardware setbacks that prevented live strain feedback in the final prototype, the concept and methodology were proven effective. The groundwork laid through my contributions offers a solid foundation for future development, especially in achieving real-time, multi-sensor strain visualization for athletic coaching tools.

Overall, my involvement in this project was integral to the successful implementation of the core sensing functionality and enabled the validation of several key performance features outlined in the initial proposal.

5.3 Future Work

Real-Time Strain Measurement Limitation

The most critical shortcoming of the project was the inability to provide real-time strain measurement and visualization. This was a direct consequence of hardware constraints, specifically the failure of the I-MON 256 High-Speed interrogator midway through the development cycle. The replacement, an older I-MON E model, was not compatible with the live data processing script originally developed for the system. Although the I-MON E device did allow for static data capture and post-processing, its CSV files were inconsistently formatted, they were "masquerading" as CSVs while containing hidden or non-standard encodings. As a result, MATLAB was unable to parse the files automatically, and our previously functioning live feedback mechanism was disabled.

The absence of real-time feedback limited the interactive value of the system in a coaching context. In future iterations, ensuring compatibility with a reliable and modern interrogator should be prioritized. . This enhancement would allow for feedback loops that update the archer in real time, potentially through a mobile or wearable interface.

Practical Usability and Fiber Routing Challenges

Another practical challenge encountered during testing was the physical routing of the optical fibers along the bow. The current configuration required fibers to extend from both the top and bottom limbs of the bow, making the system intrusive and limiting the archer's mobility. The fibers, while lightweight and sensitive, are fragile and highly susceptible to bending and signal loss if disturbed or improperly supported.

To address this, one avenue for future work involves re purposing the technology as a manufacturing or materials characterization tool. In a controlled laboratory or production setting, the fragility and routing limitations of the fiber optics become less problematic. Optical fibers with distributed FBGs could be embedded or clamped to a prototype bow to measure structural consistency during quality assurance. For example, if a standard draw force is applied across multiple bows and the measured strain differs across samples, the manufacturing consistency of limb stiffness, curvature, or lamination could be evaluated. This application could benefit composite manufacturers and bow makers seeking non-destructive, high-resolution material analysis.

Vibrational Mode Analysis with FBGs

FBG sensors can also be extended to perform vibrational analysis. Because they measure the change in periodicity at a very high temporal resolution, FBGs are sensitive to dynamic changes in the structure, including oscillations. By placing multiple FBGs along the limbs of the bow, and analyzing their time-domain strain signals through Fast Fourier Transforms (FFT), it is possible to extract the vibrational modes of the system. These vibrational signatures can then be compared against baseline healthy conditions. Deviations in vibrational profiles could indicate the presence of cracks, delamination, or other structural defects. This diagnostic capability could be valuable both for performance monitoring and structural integrity evaluation.

Incorporating Additional MPU6050 Units

Another area of expansion lies in the inertial sensing subsystem. The current implementation includes a single MPU6050 IMU placed near the grip of the bow. While this successfully captured yaw and vibrational response, it only offers a localized view of motion. By incorporating two additional MPU6050 units with one on the top limb and one on the bottom limb, it would be possible to reconstruct the motion of the entire bow during the draw and release phases.

With three IMUs, a real-time 3D reconstruction of the bow's dynamics could be achieved through sensor fusion algorithms. This setup would allow for:

- Live visualization of the bow's full-body posture in 3D space
- Detection of bending, twisting, and asymmetrical loading across limbs
- Enhanced feedback for form correction and coaching

Such a system could be integrated into virtual reality or biomechanical analysis platforms, offering even more insight into archery dynamics.

Mounting System Improvements

Lastly, the mounting system for the FBG sensors remains an area where improvement is possible. While the current design incorporates TPU for flexibility and strain transmission, fiber slippage during testing was a persistent issue. This introduced variability into strain measurements and occasionally resulted in signal loss.

Future versions of the mount could incorporate rigid PLA or epoxy-based inserts at critical clamping locations. These materials offer higher mechanical stability and can better secure the bare fiber without compressing it beyond its bend tolerance.

Conclusion

In summary, while the prototype system successfully demonstrated proof-of-concept differential strain measurement and multi-modal motion tracking, further refinement is necessary for real-world usability and broader application. Addressing the real-time feedback limitations, improving mount reliability, and exploring manufacturing or vibrational diagnostic applications represent the most promising future directions. Expanding the IMU network and integrating sensor fusion techniques could further enhance the versatility of the system, transforming it from a research prototype into a coaching and diagnostic tool.

CHAPTER 6

APPENDIX

6.1 Extension from Fall Work Term

My main accomplishment during the Fall term was the creation of a MATLAB script capable of detecting Bragg peaks in a simulated dataset and the testing done with the FBG sensors. This initial script successfully identified local maxima within a given spectrum, providing a foundation for later strain calculations. However, the system had yet to be connected to real-world data acquisition hardware, and no physical testing had been conducted. Additionally, the equation used to calculate strain at the time was based on the photelasticity model:

$$\varepsilon = \frac{\Delta\lambda_B}{\lambda_B(1 - p_e)}$$

where λ_B is the Bragg wavelength, $\Delta\lambda_B$ is the wavelength shift, and p_e is the effective photoelastic constant. This model, while theoretically accurate, requires knowledge of the photoelastic constant and real-time tracking of the original Bragg wavelength λ_B, which proved to be more complex and less practical in a dynamic application.

Algorithm Evolution and Equation Change

Perhaps the most significant change in my technical work from Fall to Winter was the evolution of the strain calculation algorithm. In the Fall, I used the photoelasticity-based equation noted above. However, as real data became available and repeatability became more important, I transitioned to a simplified model:

$$\varepsilon = \frac{\Delta\lambda}{k}$$

In this equation, k represents an empirical gauge factor that relates directly to the fiber's strain sensitivity. For standard silica fibers, $k \approx 1.2 \times 10^{-3}$ nm$/\mu\varepsilon$. The primary advantage of switching to this equation was practicality: the simplified model does not require constant recalibration or accurate knowledge of λ_B, making it far more robust in real-time applications. Given our focus on relative strain changes and differential measurements between sensors, this approach was sufficient and allowed us to detect differences in draw symmetry without over complicating the computation.

Progress During the Winter Term

In contrast, the Winter 2025 term saw substantial technical advancements, primarily through hands-on experimentation and system integration. One of the most important physical contributions was the fabrication of the FBG test bench, designed using Fusion 360 and machined from 6060 aluminum. This test bench featured two soft-padded clamps capable of gently securing bare optical fibers without damaging them. It became an essential tool for characterizing how individual FBG sensors respond to small tensile loads.

Testing on the bench enabled strain measurements to be collected for a range of fiber tensions, helping us quantify the limits of the optical fiber before signal degradation or physical failure occurred. These results informed future mounting and safety parameters. An example test involved bending a bare fiber to a radius of 5 cm. The intensity dropped significantly, as expected, due to mode loss, but no Bragg wavelength shift was observed, confirming that signal intensity, not strain, was primarily affected by sharp bends.

Throughout the semester, Yashil and I also aided in fusing two individual FBGs into a working array, which later formed the distributed sensor used in the final demonstration. This splicing process was technically challenging and involved several attempts to ensure low-loss transitions between segments. In addition to this, I performed strain testing with these fused fibers and worked closely with Yashil, who used this data to develop the final bow-mounted optical fiber support system.

Below a Gantt chart provides the major milestones throughout the semester.With the major Winter developments being: The I-MON Failure and Fall back, the Testing and completion, the testing and optimization, and the final integration and documentation.

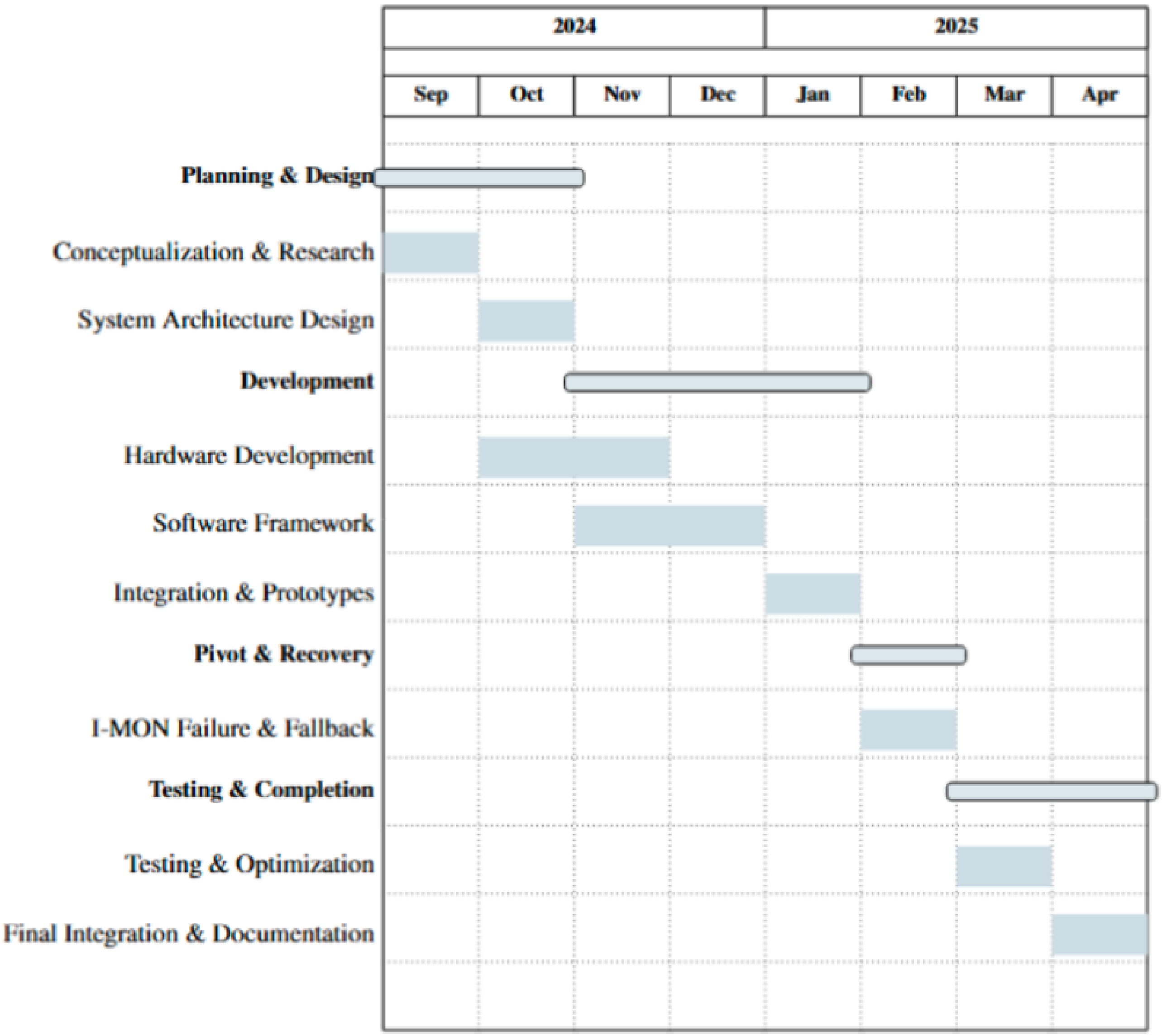

Figure 6.1: Gantt chart illustrating major milestones throughout the Winter Semester in 2025.

In summary, the Winter term represented a shift from theory to physical implementation. I developed the test bench hardware, conducted physical FBG strain testing, performed distributed sensor splicing, and refined the strain calculation algorithm based on live data. All meaningful strain measurements and spectral data used in the final report were collected during this term. The original peak detection algorithm from Fall was expanded and applied to real data, and a new mathematical model was adopted to improve reliability and usability. The technical difference between terms is clear: Fall focused on algorithm simulation, while Winter involved full system integration, physical experimentation, and deployment toward our final archery feedback tool. The reports reflect this as well.

6.2 Project Resources

Hardware Components

- 25 lbs Recurve bow
- SMF-28 optical fiber
- DenseLight DL-BP1-1501A superluminescent LED (SLED) source
- Ibsen Photonics I-MON-E USB-512 optical interrogator
- ESP32 development board
- MPU-6050 6-axis IMU
- Custom 3D-printed TPU fiber compressors and spring-loaded mounts [Yashile Thakore]

```
% Separate columns: wavelengths and counts
wavelength = data(:,1);
counts = data(:,2);

%% === Gaussian Fit ===
% Define the custom Gaussian model: y = a*exp(-((x-b)/c)^2) + d
ft = fittype('a*exp(-((x-b)/c)^2) + d', ...
             'independent', 'x', ...
             'coefficients', {'a', 'b', 'c', 'd'});

% Set initial guesses based on the data
a0 = max(counts) - min(counts);      % amplitude estimate
b0 = wavelength(counts == max(counts)); b0 = b0(1);  % center estimate (first occurrence)
c0 = 5;                              % width estimate (adjust if needed)
d0 = min(counts);                    % offset estimate

opts = fitoptions('Method', 'NonlinearLeastSquares', ...
                  'StartPoint', [a0, b0, c0, d0]);

% Fit the Gaussian model to the data
[gaussFit, gof, fit_output] = fit(wavelength, counts, ft, opts);

% Evaluate the fitted curve at the wavelength values
fit_y = gaussFit.a * exp(-((wavelength - gaussFit.b)/gaussFit.c).^2) + gaussFit.d;

%% === Plot Data and Gaussian Fit ===
figure('Name', 'Gaussian Fit', 'Color', 'w');
plot(wavelength, counts, 'bo-', 'LineWidth', 1.2); hold on;
plot(wavelength, fit_y, 'r-', 'LineWidth', 2);
xlabel('Wavelength (nm)', 'FontSize', 12);
ylabel('Counts', 'FontSize', 12);
legend('Data', 'Gaussian Fit', 'Location', 'northwest');
title('Gaussian Fit to Transmission Spectrum', 'FontSize', 14);
grid on;
box on;

%% === Calculate Residual (Peak Difference) ===
% Residual defined as the negative difference so that peaks appear positive
```

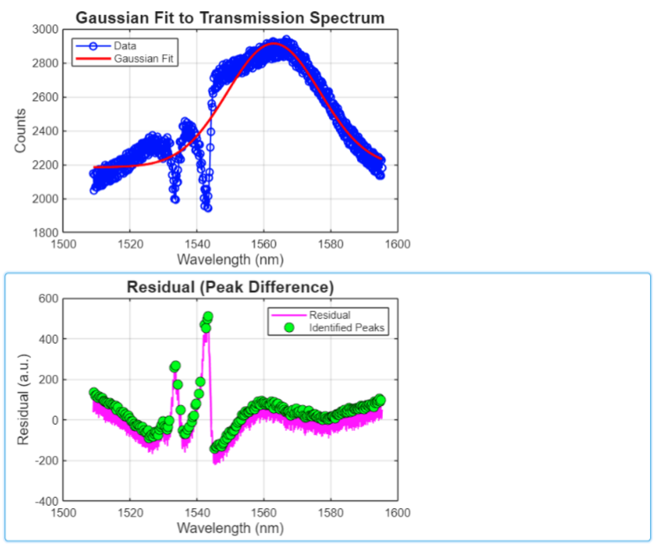

Figure 6.2: Sample Matlab Code for determining FBG Peak Locations, sample is for the same data file used in the report.

https://github.com/metehankocaman/archery-gui-capstone/

BIBLIOGRAPHY

[1]

R. Kashyap, *Fiber Bragg Gratings*, Academic Press, 1999.

[2]

A. Othonos and K. Kalli, *Fiber Bragg Gratings: Fundamentals and Applications in Telecommunications and Sensing*, Artech House, 1999.

[3]

Martins, M *Fiber Bragg Gratings: Theory and Practice*, 2nd ed., Academic Press, 2010.

[4]

W. J. Palm III, *Introduction to MATLAB for Engineers*, 2nd ed., McGraw-Hill, 2009.

[5]

Ibsen Photonics, *I-MON E Interrogator 512 User Manual*, Ibsen Photonics, 2024.

[6]

W. H. Press, S. A. Teukolsky, W. T. Vetterling, and B. P. Flannery, *Numerical Recipes: The Art of Scientific Computing*, 3rd ed., Cambridge University Press, 2007.